



Identification of the appropriate dose metric for pulmonary inflammation of silver nanoparticles in an inhalation toxicity study

Hedwig M. Braakhuis, Flemming R. Cassee, Paul H.B. Fokkens, Liset J.J. de la Fonteyne, Agnes G. Oomen, Petra Krystek, Wim H. de Jong, Henk van Loveren & Margriet V.D.Z. Park

To cite this article: Hedwig M. Braakhuis, Flemming R. Cassee, Paul H.B. Fokkens, Liset J.J. de la Fonteyne, Agnes G. Oomen, Petra Krystek, Wim H. de Jong, Henk van Loveren & Margriet V.D.Z. Park (2016) Identification of the appropriate dose metric for pulmonary inflammation of silver nanoparticles in an inhalation toxicity study, *Nanotoxicology*, 10:1, 63-73, DOI: [10.3109/17435390.2015.1012184](https://doi.org/10.3109/17435390.2015.1012184)

To link to this article: <http://dx.doi.org/10.3109/17435390.2015.1012184>



View supplementary material [↗](#)



Published online: 23 Feb 2015.



Submit your article to this journal [↗](#)



Article views: 407



View related articles [↗](#)



View Crossmark data [↗](#)



Citing articles: 9 View citing articles [↗](#)

ORIGINAL ARTICLE

Identification of the appropriate dose metric for pulmonary inflammation of silver nanoparticles in an inhalation toxicity study

Hedwig M. Braakhuis^{1,2}, Flemming R. Cassee^{2,3}, Paul H.B. Fokkens², Liset J.J. de la Fonteyne², Agnes G. Oomen², Petra Krystek⁴, Wim H. de Jong², Henk van Loveren^{1,2}, and Margriet V.D.Z. Park²

¹Department of Toxicogenomics, Maastricht University, Maastricht, The Netherlands, ²Centre for Health Protection, Centre for Sustainability, Environment and Health, Centre for Safety of Substances and Products, National Institute for Public Health and the Environment (RIVM), Bilthoven, The Netherlands, ³Environmental Epidemiology, Institute of Risk Assessment Sciences, Utrecht University, TD Utrecht, The Netherlands, and ⁴Philips Innovation Services, Eindhoven, The Netherlands

Abstract

A number of studies have shown that induction of pulmonary toxicity by nanoparticles of the same chemical composition depends on particle size, which is likely in part due to differences in lung deposition. Particle size mostly determines whether nanoparticles reach the alveoli, and where they might induce toxicity. For the risk assessment of nanomaterials, there is need for a suitable dose metric that accounts for differences in effects between different sized nanoparticles of the same chemical composition. The aim of the present study is to determine the most suitable dose metric to describe the effects of silver nanoparticles after short-term inhalation. Rats were exposed to different concentrations (ranging from 41 to 1105 µg silver/m³ air) of 18, 34, 60 and 160 nm silver particles for four consecutive days and sacrificed at 24 h and 7 days after exposure. We observed a concentration-dependent increase in pulmonary toxicity parameters like cell counts and pro-inflammatory cytokines in the bronchoalveolar lavage fluid. All results were analysed using the measured exposure concentrations in air, the measured internal dose in the lung and the estimated alveolar dose. In addition, we analysed the results based on mass, particle number and particle surface area. Our study indicates that using the particle surface area as a dose metric in the alveoli, the dose–response effects of the different silver particle sizes overlap for most pulmonary toxicity parameters. We conclude that the alveolar dose expressed as particle surface area is the most suitable dose metric to describe the toxicity of silver nanoparticles after inhalation.

Keywords

Dose metrics, inhalation exposure, nanotoxicology, risk assessment

History

Received 15 August 2014

Revised 14 January 2015

Accepted 20 January 2015

Published online 23 February 2015

Introduction

Nanomaterials are composed of primary and agglomerated particles that can vary in size, shape, charge, crystallinity, chemical composition and other characteristics, and this variety will increase even further in the future (SCENIHR, 2010). Of these characteristics, size has been put forward as an essential parameter to predict the pulmonary inflammation caused by nanomaterials (Duffin et al., 2007; Horie et al., 2012; Kobayashi et al., 2009; Oberdorster et al., 2000; Stoeger et al., 2006), although many other factors also modulate the outcome of toxicity studies (Bakand et al., 2012; Braakhuis et al., 2014b; Cho et al., 2012; Landsiedel et al., 2010; Ma-Hock et al., 2013; Schinwald et al., 2012; van Ravenzwaay et al., 2009; Warheit et al., 2007a,b). In inhalation studies using similar mass exposure concentrations of microparticles (>1 µm) and nanoparticles, differences in effects may be the result of differences in total surface area and total

particle number, but also in lung deposition and clearance (Asgharian et al., 2009). In a recent study, silver nanoparticles of two different sizes showed a clear size-dependent effect after short-term *in vivo* inhalation; 15 nm particles induced moderate pulmonary toxicity while 410 nm particles did not (Braakhuis et al., 2014a). The observed effects were likely caused by the difference in the internal alveolar dose between the 15 and 410 nm silver particles and by the release of silver ions from the (nano)particle surface. Several other *in vivo* studies also showed that smaller nanoparticles caused more pronounced adverse effects after inhalation compared to larger particles of the same chemical composition when applying the same mass concentrations (Duffin et al., 2007; Horie et al., 2012; Kobayashi et al., 2009; Oberdorster et al., 2000; Stoeger et al., 2006). For nanoparticles studied in those experiments, the deposited particle surface area seems to be a better predictor for the induction of pulmonary inflammation than mass exposure concentrations. In other *in vivo* studies no correlations between decreasing primary particle size and increasing pulmonary inflammation were obtained (Gosens et al., 2014; Pauluhn, 2009; Roursgaard et al., 2010; Warheit et al., 2006; Zhu et al., 2008). In two of these studies, the agglomerate particle size was similar for particles of different primary size, resulting in similar deposition patterns in the lungs (Gosens et al., 2014; Pauluhn, 2009) and

Correspondence: Hedwig Braakhuis, MSc, Centre for Health Protection, RIVM – National Institute for Public Health and the Environment, PO Box 1, 3720 BA Bilthoven, The Netherlands. Tel: +31 30 274 41 72. E-mail: hedwig.braakhuis@rivm.nl

possibly explaining the absence of a primary particle size related effect.

For risk assessment purposes, for example, to derive exposure limits, there is need for a suitable dose metric of nanomaterials that accounts for differences in effects between different sized nanoparticles of the same chemical composition. In the present study, we chose to focus on silver nanoparticles as these are currently the most commonly mentioned in product descriptions because of their antimicrobial activity (Nanotechnologies, 2014; Wijnhoven et al., 2009). The aim of this study is to determine the most suitable dose metric to describe the effect of silver nanoparticles after inhalation irrespective of the size of the primary particle. From previous studies, it is known that silver nanoparticles can release silver ions from their surface (Kent & Vikesland, 2012; Leo et al., 2013; Ma et al., 2012; Stebounova et al., 2011; Zook et al., 2011) that contribute to the observed toxicity after inhalation (Beer et al., 2012; Pratsinis et al., 2013; Wang et al., 2014). Because of their high surface to volume ratio and the release of silver ions from the surface, we hypothesize that deposited particle surface area might be a suitable dose metric to predict the pulmonary toxicity of silver nanoparticles after inhalation.

To address this hypothesis, rats were exposed by inhalation to four different concentrations of 18, 34, 60 and 160 nm silver (nano)particles for four consecutive days to obtain dose–response data. We measured the total lung burden and estimated the alveolar dose using a multiple path particle dosimetry (MPPD) model (Asgharian et al., 2009). We subsequently correlated various dose metrics with a suit of toxicity markers determined at 24 h and 7 days after the last exposure.

Methods

Test material generation

The test atmosphere was produced by mixing silver nanoparticles with HEPA filtered and conditioned (50% RH, 21 °C) compressed air. The silver nanoparticles were produced by a Palas GFG 1000 (Palas GmbH, Karlsruhe, Germany) spark generator fitted with silver tipped electrodes. To generate the smallest aerosol size (15–20 nm CMD), the output of the generator was immediately diluted in conditioned air. To generate the two intermediate aerosol sizes of 30–35 nm and 60–65 nm, a longer residence time of spark generated particles in mixing chambers was used to lead the aerosol into the exposure chamber. This increased residence time resulted in aggregation, which is a function of time. In order to obtain spherical particles, the aerosol was heated by passing it *via* tubing through an oven at 700 °C, which resulted in fusing of aggregates. Oxygen was added to the dilution and cooled air to a final concentration of 20%. The particle number concentration was controlled by the spark generator frequency. The final condition of the aerosol (55% RH, 21 °C) was set by adjusting the relative humidity of the mixing air. It is not possible to use this spark generation method to produce silver nanoparticles larger than 60–65 nm. Therefore, we used another generation method to generate larger silver nanoparticles.

Silver particles (80 nm) were purchased from NanoComposix, Inc. (San Diego, CA). The 80 nm silver particles were polyvinylpyrrolidone (PVP)-coated and supplied in solution of 1 mg/ml in MilliQ water. The silver particle suspension was passed through a small nozzle of a Schlick spray nozzle (Düsen-Schlick GmbH, Untersiemau/Coburg, Germany) to obtain an aerosol. The nebulized particles were mixed with compressed air in a heated mixing tube. After mixing and passing the aerosol through a diffusion dryer to get rid of the water, the aerosol was passed through an oven as described above. At temperatures above 500 °C, PVP completely decomposes (Du et al., 2006;

Peniche et al., 1993). The high temperature of 700 °C removed the PVP-coating of the silver particles. After the oven, the aerosol was diluted with conditioned air and cooled down. The final condition of the aerosol (55% RH, 21 °C) was set by adjusting the relative humidity.

Test atmosphere characterization

The particle mass concentration was determined by gravimetric analysis of particles collected on Teflon R2PJ047 filter (Pall Corp., Ann Arbor, MI). Mass concentrations were also monitored using a tapered element oscillating microbalance (TEOM) series 1400 (Rupprecht & Patashnick, New York). The particle number concentration was measured by a condensation particle counter CPC 3022 (TSI Inc., St. Paul, MN). Particle size distribution was monitored by an optical particle sizer (OPS) 3330 (TSI Inc., St. Paul, MN), a scanning mobility particle sizer (SMPS) 3080 with 3085 Nano differential mobility analyser (DMA) (TSI Inc., St. Paul, MN) and a micro-orifice impactor (MOI) Model No. 110 (MSP Corp, Minneapolis, MN). Temperature and relative humidity were determined continuously during the exposures using a Vaisala M170 (Vaisala Oyj, Helsinki, Finland). The particle size and spherical appearance were confirmed by scanning electron microscopy (SEM) using a Nova Nanolab 600 Dualbeam (FEI, Eindhoven, The Netherlands), about 300 particles per particle size were analysed using SEM. The measurements of particle mass, number and particle size (count median diameter) were used to estimate the particle surface area in the external exposure air. This is assuming that the particles were spherical, which was confirmed by the SEM images of the particles (Figure S1). For the internal doses, we measured the mass of the silver present in the lungs with high-resolution inductively coupled plasma mass spectrometry (HR-ICP-MS). In combination with the particle size measured during exposure, we could estimate the particle surface area. For the alveolar dose, we used the MPPD model to estimate the mass fraction that would reach the alveoli and used the HR-ICP-MS results to calculate the mass that would reach the alveoli. Again, by using the particle size in combination with the mass we could estimate the particle surface area.

Animals

Male Fischer rats (F344/DuCrI), specific pathogen free (SPF) were supplied by Charles River (Sulzfeld, Germany). After an acclimatization period of two weeks, the animals were 10 weeks old at the start of the experiment. All animals were free from clinical signs of disease. The rats were randomly allocated to the control and the test groups. During exposure, the animals were restrained in nose-only tubes (CH Technologies, Westwood, NJ) fixed to the inhalation system. When not exposed, animals were housed up to three animals in macrolon III cages with filtertops to prevent dust entering the cages (bedding material: Lignocel S8-15, Altromin Spezialfutter GmbH & Co. KG, Germany). The animals' room was air-conditioned with a 12 h light–12 h dark cycle, the temperature ranging from 20 to 24 °C with relative humidity ranging from 30% to 70%. Except during exposure, certified feed CRM (SDS Diets, Essex, UK) and water were available *ad libitum*. Before start of the exposure period, all animals were acclimatized to the nose only tubes for three consecutive days for 1 h per day. At 24 h and 7 days after the last exposure, rats were weighed, anesthetized by a single intraperitoneal injection of ketamine (75 mg/kg) and xylazine (10 mg/kg) and subsequently exsanguinated *via* the abdominal aorta. Husbandry conditions were maintained according to all applicable provisions of the national laws, Experiments on Animals Decree and Experiments on Animals Act.

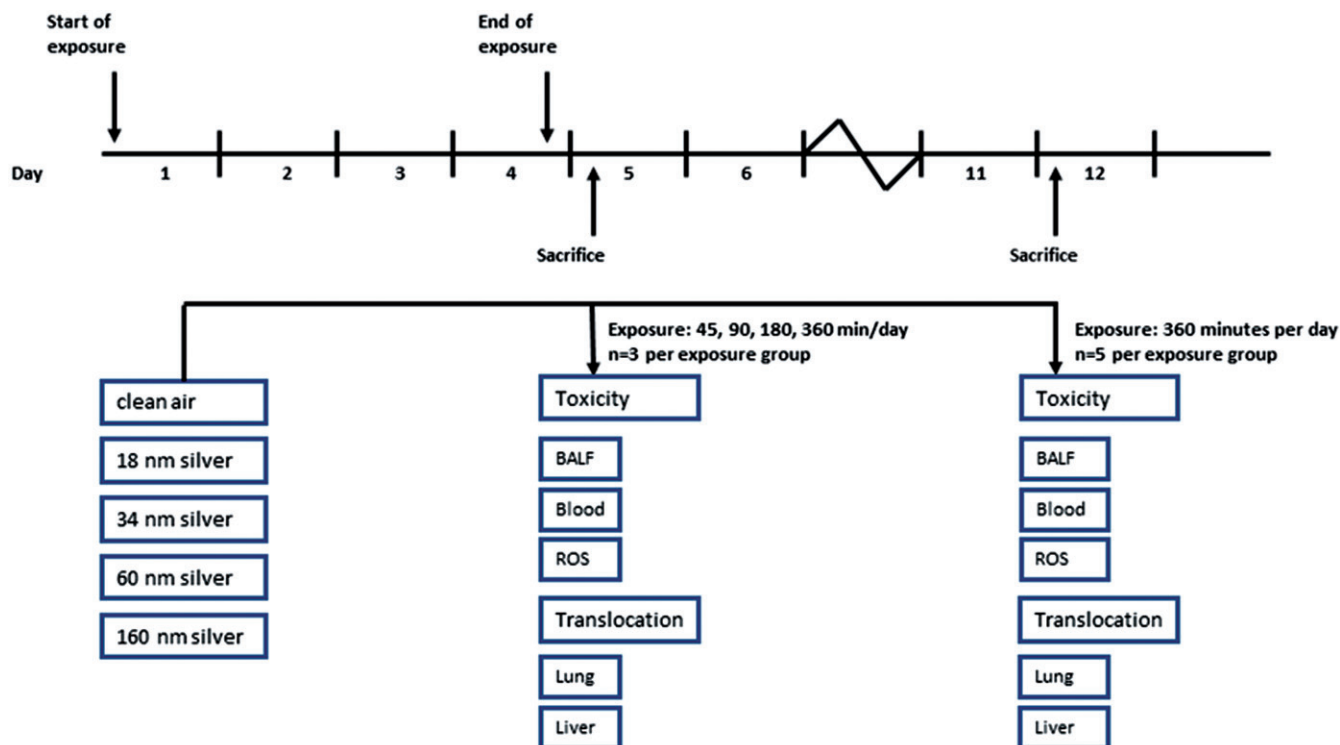


Figure 1. Experimental design of the short-term inhalation study. Rats were nose-only exposed for 45 min, 90 min, 3 h or 6 h per day for four consecutive days to particle free air, or atmospheres containing either 18, 34, 60 or 160 nm silver nanoparticles, three rats per group. All rats were sacrificed 24 h after exposure to determine the induction of pulmonary toxicity and the tissue distribution. In addition, rats were exposed for 6 h per day for four consecutive days to either clean air or silver nanoparticles, five rats per group, and sacrificed 7 days after exposure.

Experimental design

The experiments were conducted at the National Institute for Public Health and the Environment (RIVM, Bilthoven, The Netherlands) according to a protocol approved by the local Ethics Committee for Animal Experiments and according to European and national laws regulating the use of laboratory animals. The experimental design is shown in Figure 1. To obtain dose-response data, rats were exposed to different concentrations of the silver (nano)particles by exposing them during different lengths of time. Rats were nose-only exposed for 45 min, 90 min, 3 h or 6 h per day for four consecutive days to particle free air, or atmospheres containing either 18, 34, 60 or 160 nm silver nanoparticles, three rats per group. All rats were sacrificed 24 h after exposure to determine the induction of pulmonary toxicity and the tissue distribution. Besides the dose-response data, we investigated whether possible effects were persistent. Per particle size, rats were exposed for 6 h per day for four consecutive days to either clean air or silver nanoparticles, five rats per group and sacrificed 7 days after exposure.

Quantification of silver in tissues by high-resolution inductively coupled plasma mass spectrometry

The presence of silver in the left lung and liver was determined by high-resolution inductively coupled plasma mass spectrometry (HR-ICP-MS) (Krystek, 2012; Krystek et al., 2013). In the other collected organs (spleen, kidneys, testis and brain), we did not measure the level of silver because the amount of silver in these organs was expected to be below the detection limit of 0.01 µg/g tissue based on previous finding using 15 and 410 nm silver particles (Braakhuis et al., 2014a). Samples of homogenized tissue (max. 0.5 g) were completely dissolved on a block heater (Stuart SBH200D, supplied by Omnilabo, Breda, The Netherlands) for 24 h at 120 °C after the direct addition of aqua

regia (0.5 ml 60% nitric acid, ultrapure and 1.5 ml 30% hydrochloric acid, ultrapure; Merck, Darmstadt, Germany) and afterwards diluted. The silver concentration in the digests was determined using high-resolution inductively coupled plasma mass spectrometry (HR-ICPMS; Element XR, Thermo Fisher Scientific, Bremen, Germany). External calibration curves of the interference-free silver isotopes were used for quantification. Both silver isotopes (^{107}Ag and ^{109}Ag) were measured in the low-resolution mode. On-line addition and correction with an internal standard (rhodium with the measured isotope ^{103}Rh in the low-resolution mode) was applied as well. The results of ^{107}Ag were reported and the results of ^{109}Ag were used for control. Sample pre-treatment and analysis were carried out in a cleanroom facility class 100 000.

Estimated deposited dose in lungs using multiple path particle dosimetry (MPPD) model

To estimate the fractions of deposited dose in the head, tracheobronchial and alveolar region of the rats, the latest online version of the multiple path particle dosimetry model V2.11 (MPPD model) was used (Asgharian et al., 2009; Cassee et al., 2002) (<http://www.ara.com/products/mppd.htm>). We used the default parameters of the model for rats, i.e. a forced respiratory capacity of 4 ml, head volume of 0.42 ml, nasal breathing, tidal volume of 2.1 ml and a breathing frequency of 102/min (Anjilvel & Asgharian, 1995; Asgharian et al., 2009; Yeh et al., 1979). The inspiratory fraction was 0.5, and no pause was entered. Calculations were done using the count median diameter (CMD), geometric SD, the mass concentration and a density of 10.49 g/cm³. Calculations included both deposition of the silver nanoparticles in various regions of the respiratory system (extra-thoracic, tracheobronchial and pulmonary region) and the estimated clearance.

Clinical examinations

The animals were examined once daily throughout the study period. On exposure days, the animals were examined three times per day (before, during and after exposure). The clinical examination included examination of attitude, animal fur, activity level, food and water intake, and faeces and urine production. The body weight of the animals was determined at arrival, at the start of the exposure period and at the day of sacrifice.

Haematology analysis

Blood samples were collected in K3EDTA-containing tubes for the analysis of cell types and concentrations (ADVIA 120 Hematology Analyzer, Siemens, Deerfield, IL), and in citrate vials for analysis of inflammatory markers in the blood. The level of fibrinogen in the citrate plasma was measured using a rat fibrinogen ELISA kit (GenWay Biotech, Inc., San Diego) according to manufacturer's instructions.

Bronchoalveolar lavage analysis

The left lung of the rats was bound just below the bifurcation of the trachea and the right lung was cannulated *via* the trachea. Bronchoalveolar lavage was performed *in situ* by infusing the right lung three times with 27 ml/kg physiological saline. The retrieved bronchoalveolar lavage fluid (BALF) was kept on ice and centrifuged for 10 min at 400 *g*. The pellet was suspended in physiological saline for analysis of the total cell number (Coulter Counter Z2, Coulter Electronics, Mijdrecht, The Netherlands) and cell differentials. Cytospin preparations were stained according to May-Grünwald and Giemsa and evaluated microscopically for macrophages, polynuclear macrophages, neutrophils, lymphocytes, monocytes and eosinophils. At least 400 cells were counted, 200 cells per slide. The cell-free supernatant was collected to assess cell damage by measurement of total protein content and the release of lactate dehydrogenase (LDH) by Beckman Coulter autoanalyser Unicel DxC800 Clinical Systems (Beckman Coulter, Inc.), and to assess the induction of pro-inflammatory cytokines. The remainder of the supernatant was stored at -80°C .

Measurement of pro-inflammatory cytokines

The presence of pro-inflammatory cytokines IL-1 β , IL-6, TNF- α , GM-CSF, MCP-1, IL-12p70, MIP-2 and RANTES in the supernatant of the BALF was measured by a Bio-Plex Pro assay for rat cytokines according to manufacturer's instructions (Bio-Rad Laboratories, Inc.).

Measurement of oxidative stress

The induction of oxidative stress was determined by measuring the amount of reduced, oxidized and total glutathione in the lungs. The rinsed right lung was homogenized on ice in 4 ml of phosphate buffer (pH 7.2). Subsequently, the homogenate was centrifuged at 600 *g* for 10 min. To extract the proteins from the samples, the supernatant was mixed 1:1 with metaphosphoric acid, incubated for 15 min on ice, and centrifuged at 4000 rpm for 10 min. The amount of reduced, oxidized and total glutathione was measured by Beckmann Coulter Autoanalyser (Beckman Coulter, Inc.) in the supernatant.

Dose metrics

The dose–response data was analysed using different dose metrics to determine the most suitable dose metric to describe the effects of silver nanoparticles after inhalation. The exposure was

analysed in three different ways: (1) as the external silver concentration in air, measured during exposure, (2) as the internal lung dose of silver, measured by HR-ICP-MS and (3) as the alveolar dose, calculated using the exposure concentration and the internal lung dose in combination with the MPPD model. In addition, the data was visualized and analysed based on mass, particle number and total surface area for the external, internal and alveolar dose. In total, nine different graphs were produced and analysed for each chosen effect parameter. In the graphs representing the internal lung and alveolar dose, the dose is different for each animal.

Statistical analysis

The raw data of the BALF was corrected for retrieved fluid. All experimental data were combined in one dataset, which was analysed using the dose-response modelling software PROAST (RIVM, Bilthoven, The Netherlands) (RIVM, 2014; Slob, 2002), according to methods described earlier (Park et al., 2009). PROAST is a benchmark dose software that can be used for dose–response analysis (Barlow et al., 2009; EFSA, 2009). Briefly, the PROAST software selects the optimal data fitting model from an exponential family of models using the likelihood-ratio criterion (Slob, 2002). To correct for the different within-group variances between the different exposure groups, the data was log-transformed (Slob, 2014a,b). For the comparison of particles, the particle identification (18, 34, 60, 160) was defined as a covariate, which reflects the potency of the administered agent. A *p* value of <0.05 for the associated likelihood-ratio test was considered as a statistically significant effect of particle size. The potential differences between particle sizes was further quantified by the critical effect dose of silver nanoparticles CED_{20} , defined as the (nominal) dose resulting in a 20% response compared to the control group. We chose a critical effect size of 20% based on the magnitude of effect in previous studies with ambient particulate matter or nanoparticles (Gerlofs-Nijland et al., 2007; Gosens et al., 2014; Stoeger et al., 2006) and expert judgement on physiologically relevant changes. In addition, the data was analysed by the Kruskal–Wallis nonparametric test (Graphpad Prism). Statistical significance is indicated with a $*$ ($p \leq 0.05$). In all graphs, error bars represent the standard deviation of the mean.

Results

Nanoparticle characteristics

The particle characteristics are summarized in Table 1. The generated particle sizes were 18.1 nm (GSD 1.24), 34.5 nm (GSD 1.30), 60.3 nm (GSD 1.32) and 160 nm (GSD 1.55) and confirmed by SEM (Figure S1). The 160 nm particles probably consisted of three to five agglomerated silver nanoparticles of 80 nm that were fused into single spherical particles in the oven. The exposure mass concentrations were similar for the particles of 18, 34 and 60 nm and about three times higher for the 160 nm particles to obtain total particle surface area concentrations in the same range. The particle size distributions and number concentrations are shown in Figure S2.

Quantification of silver in lung and liver by HR-ICP-MS

In both the lungs and the liver, the level of silver showed a concentration-dependent increase at 24 h after exposure. The level of silver measured in the left lung was normalized to the total lung weight to calculate the total amount of silver in the lungs. For the highest concentration tested, the total lung deposition of silver was 25.5 μg of the 18 nm particles, 33.0 μg of the 34 nm particles, 40.0 μg of the 60 nm particles and 46.1 μg of the 160 nm particles (Figure 2). At 7 days after exposure, the amount of silver in the

Table 1. Nanoparticle characteristics. Particle size is given as count median diameter (CMD) with the geometric standard deviation (GSD). Mass, particle number and surface area shown as mean (SD).

Agglomerate size (nm)	Mass ($\mu\text{g}/\text{m}^3$)	Particle number ($\#/\text{cm}^3$)	Surface area (nm^2/cm^3)
18.1 (1.24)	438 (130)	1.3×10^7 (4.0×10^6)	1.4×10^{10} (4.1×10^9)
34.5 (1.3)	325 (50)	6.6×10^6 (1.0×10^5)	5.4×10^9 (9.0×10^8)
60.3 (1.32)	341 (21)	3.6×10^5 (2.1×10^4)	3.2×10^9 (1.1×10^8)
160 (1.55)	1109 (46)	5.3×10^4 (1.7×10^3)	1.4×10^9 (4.3×10^8)

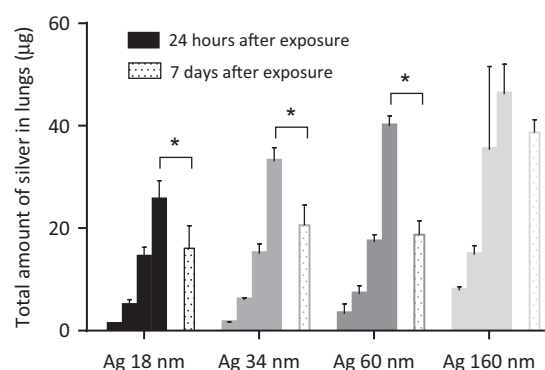


Figure 2. Amount of silver detected in the lungs by HR-ICP-MS at 24 h and 7 days after exposure. Columns show doses administered from left to right based on control air, and 45 min, 90 min, 3 h or 6 h inhalation exposure to silver nanoparticles per day. At 24 h after exposure, the level of silver in the lungs correlated with the exposure concentrations, showing a dose-response with increasing total lung deposition upon increasing exposure concentrations. *For the 18, 34 and 60 nm particles, the amount of silver in the lungs at 7 days after exposure was significantly lower compared to 24 h after exposure ($p < 0.05$, $p < 0.01$, $p < 0.0001$, respectively).

lungs decreased to 16.1 μg for the 18 nm particles, 20.6 μg for the 34 nm particles, 18.7 μg for the 60 nm particles and 38.7 μg for the 160 nm particles. The clearance from the lungs was the lowest for the 160 nm particles; about 16% of the total mass burden was cleared at 7 days after exposure compared to a clearance of about 37% for the 18 and 34 nm particles and even 53% for the 60 nm particles. In the liver, the amount of detected silver was 0.52 μg for the 18 nm particles, 0.75 μg for the 34 nm particles, 0.71 μg for the 60 nm particles and 0.24 μg for the 160 nm particles for the highest concentration tested at 24 h after exposure. Compared to the total lung burden, the relative amount of silver in the liver was the highest for the 34 nm particles and the lowest for the 160 nm particles (Figure 3). The fraction of total deposited silver in the lungs that reached the liver decreased with increasing total lung burden. At 7 days after exposure, the level of silver in the liver decreased to 0.07, 0.31, 0.17 and 0.17 μg for the 18, 34, 60 and 160 nm particles, respectively.

Estimated deposited alveolar dose in lungs using multiple path particle dosimetry model

According to the multiple path particle dosimetry (MPPD) model, the deposited fraction of the inhaled dose of the silver nanoparticles in the tracheobronchial and alveolar region of the lungs was 0.66 for the 18 nm particles, 0.5 for the 34 nm particles, 0.37 for the 60 nm particles and 0.39 for the 160 nm particles. The remaining fraction can be exhaled or may deposit in the nasal cavity. For the alveolar region, the deposition fraction is 0.28 for both the 18 and 34 nm particles, 0.22 for the 60 nm particles and 0.10 for the 160 nm particles. Based on the exposure concentration and the HR-ICP-MS results in combination with the MPPD

model, we estimated the deposited dose in the alveolar region. Based on mass, the alveolar dose was calculated to be 11 μg for the 18 nm particles, 19 μg for the 34 nm particles, 24 μg for the 60 nm particles and 12 μg for the 160 nm particles for the highest concentration tested at 24 h after exposure (Figure 4). This equals to a particle number of 2.1×10^{11} , 5.3×10^{10} , 1.2×10^{10} and 4.1×10^8 per cm^3 , respectively. The estimated particle surface area dose in the alveoli is 2.2×10^{14} , 1.9×10^{14} , 1.4×10^{14} and 3.3×10^{13} nm^2/cm^3 for the 18, 34, 60 and 160 nm particles, respectively, at the highest concentration tested at 24 h after exposure. When expressed as mass, the internal alveolar dose is does not differ that much between the different particle sizes. When expressed as particle number or particle surface area, the internal alveolar dose is much higher for the smaller particles compared to the larger particles. For the 18 nm particles, the particle number in the alveoli is about 510 times higher compared to the 160 nm particles and the particle surface area is about 6.5 times higher.

Clinical examinations

Exposure to silver nanoparticles of 18, 34, 60 and 160 nm did not induce any premature mortality. There were no effects on animal attitude, fur, activity pattern, food and water consumption and faeces and urine production, and no effects on body weights and organ weights throughout the study (Table S1).

Haematology

In blood, measured parameters (erythrocytes, leukocytes, leukocyte differentiation, platelets and reticulocytes, haemoglobin, haematocrit, MCV, MCH and MCHC) did not change at 24 h or 7 days after exposure to silver nanoparticles (data not shown). There were no differences in the haematological endpoints among the groups of rats exposed to the different particle sizes. In addition, there were no differences detected in the level of fibrinogen in the plasma between the controls and the exposed animals (data not shown).

Total cell counts and differential cell counts in the bronchoalveolar lavage fluid (BALF)

For all particle sizes, the total cell number showed a concentration-dependent increase at 24 h after the end of the exposure period. The increased total cell number was mainly caused by a neutrophil influx (Figure S3). The number of neutrophils increased exposure concentration dependently for all particle sizes. For the 18 and the 34 nm silver nanoparticles, the number of lymphocytes and monocytes also showed a concentration-dependent increase at 24 h after exposure. For the 60 and 160 nm particles, there was no increase of lymphocytes and monocytes. The number of macrophages and eosinophils was not affected by the exposure to silver nanoparticles at 24 h after exposure (data not shown).

At 7 days after exposure, the total cell number decreased for all particle sizes compared to 24 h after exposure. However, for the animals exposed to 60 nm silver nanoparticles, the total cell

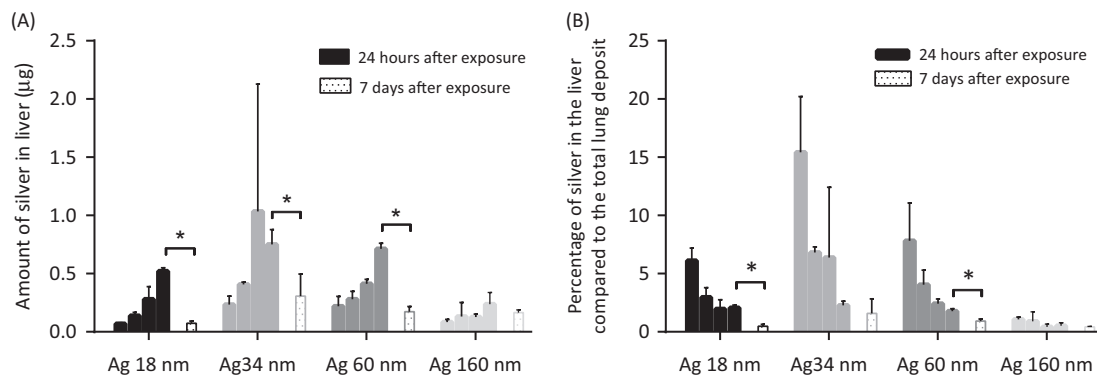


Figure 3. Amount of silver detected in the liver by HR-ICP-MS at 24 h and 7 days after exposure, expressed as total amount of silver (A) and as percentage of the deposited dose in the lungs (B). The total amount of silver in the liver showed an increase upon increasing exposure concentrations in air (A). *For the 18, 34 and 60 nm particles, the total amount of silver in the liver at 7 days after exposure was significantly lower compared to 24 h after exposure ($p < 0.001$ for all three particle sizes). When expressed as fraction of the deposited dose in the lungs, smaller fractions of silver reach the liver upon increasing deposited doses in the lungs (B). *For the 18 and 60 nm particles, the fraction of silver in the liver at 7 days after exposure was significantly lower compared to 24 h after exposure ($p < 0.01$ for both particle sizes).

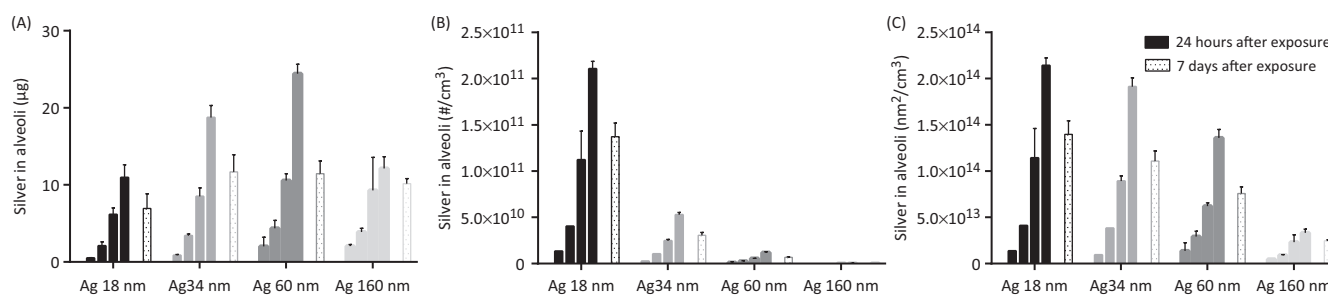


Figure 4. Estimated amount of silver in the alveoli based on the exposure concentrations, HR-ICP-MS measurements and the MPPD model. Results are shown as the estimated mass (A), particle number (B) and particle surface area (C) in the alveoli. Columns show doses administered from left to right based on control air, and 45 min, 90 min, 3 h or 6 h inhalation exposure to silver nanoparticles per day.

number was still significantly increased compared to the controls ($p < 0.05$) (Figure S4). Although the number of neutrophils decreased at 7 days after exposure compared to 24 h after exposure, for the animals exposed to 34 and 60 nm silver nanoparticles the number of neutrophils was still significantly increased compared to the controls ($p < 0.001$ and $p < 0.01$, respectively). In addition, the number of lymphocytes in the BALF was significantly increased in the animals exposed to 34 and 60 nm silver nanoparticles at 7 days after exposure compared to the controls ($p < 0.01$ and $p < 0.05$, respectively). There was no significant difference between the exposed groups and the controls in the number of macrophages and monocytes at 7 days after exposure. These results show a prolonged inflammation in the lungs after exposure to 34 and 60 nm silver nanoparticles.

LDH and total protein in the BALF

Exposure to 18 and 34 nm silver nanoparticles induced an exposure concentration dependent increase in LDH and total protein in the BALF, indicating the induction of cellular damage in the lungs at 24 h after exposure. Exposure to 60 and 160 nm silver particles did not induce an increase in LDH and total protein in the BALF at 24 h after exposure (Figure 5). At 7 days after exposure, both the levels of LDH and total protein decreased. The level of LDH in animals exposed to 34 nm silver nanoparticles was still significantly increased compared to the controls ($p < 0.05$). The level of total protein did not significantly differ between the controls and the exposed groups at 7 days after exposure.

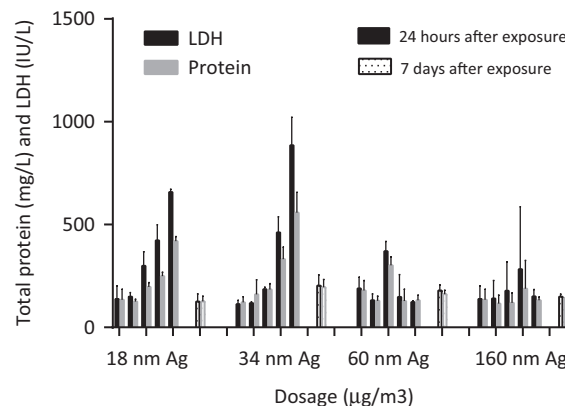


Figure 5. The level of protein and LDH in the BALF at 24 h and 7 days after exposure to different sizes of silver nanoparticles based on the mass exposure concentrations. Exposure to 18 and 34 nm silver particles induced an exposure concentration-dependent increase in the level of protein and LDH in the BALF, whereas exposure to 60 and 160 nm silver particles do not. Columns show doses administered from left to right based on control air, and 45 min, 90 min, 3 h or 6 h inhalation exposure to silver nanoparticles per day.

Pro-inflammatory cytokines in the BALF

Of the selected cytokines, IL-1 β , TNF- α , MCP-1 and RANTES showed an exposure concentration-dependent increase for all particle sizes. The results of IL-1 β and MCP-1 are shown in Figure S5. IL-6, IL-12p70 and GM-CSF were below the detection limit.

MIP-2 was detectable, but did not correlate with the exposure to silver particles.

Oxidative stress in the lungs

The induction of oxidative stress was determined by measuring the level of glutathione in the lungs of the rats exposed to silver nanoparticles. The level of total glutathione did not differ between the controls and the exposed groups. In addition, exposure to silver nanoparticles did not induce any significant changes in the level of reduced (GSH) and oxidized (GSSG) glutathione. The ratio of GSH/GSSG was also not affected by the exposure to silver nanoparticles (data not shown).

Dose metrics

We selected the total cell number, the number of neutrophils, and the level of IL-1 β and MCP-1 in the lung fluid at 24 h after the end of the exposure period to determine the most suitable dose metric for silver nanoparticles after inhalation as these were significantly affected by the test atmospheres. The data was analysed using (1) the external silver concentration in air as measured during exposure, (2) the internal lung dose of silver as measured by HR-ICP-MS and (3) the alveolar dose as calculated using the exposure concentration and the internal lung dose in combination with the MPPD model. In addition, the data is graphically presented based on mass, particle number and total surface area for external, internal and alveolar dose. For each of the chosen effect parameters, nine different graphs were produced (Figure 6) and they all showed that when the particle surface area that reaches the alveoli is used as a dose metric, the dose–response curves of the various particle sizes almost completely overlap (Figure 7). Using PROAST software, we calculated the critical effect concentration or dose (CED) that would induce a 20% response compared to the unexposed control animals (CED₂₀) (Figure 8). Based on the exposure concentration, the CED₂₀ of the different sized silver nanoparticles do not overlap when expressed as mass or particle number. When expressed as surface area, the critical effect concentrations are more close to each other, but do not overlap. The same happens for the internal dose in the lungs; mass and particle number doses result in different CED₂₀ for the different particle sizes, while surface area brings them more towards each other. Based on the alveolar dose, however, the CED₂₀ of the different particle sizes do overlap when the dose is expressed as surface area (Figure 8). Therefore, in the alveoli, particle surface area seems the best dose metric to describe the effect of silver nanoparticles on the total cell number, the number of neutrophils and the level of IL-1 β and MCP-1 after short-term inhalation.

Discussion

The results of the present study show that after short-term exposure by inhalation the effects of silver nanoparticles (based on a set of markers for inflammation) can best be predicted by the total surface area of the silver nanoparticles that reach the alveoli. There are several reasons why the alveolar dose expressed as particle surface area is a suitable dose descriptor for the pulmonary toxicity of silver nanoparticles. (1) The alveoli are the site of the observed toxicity. (2) Silver nanoparticles of different sizes have a different deposition pattern in the lungs, including the alveoli. (3) Silver nanoparticles can release silver ions from their surface, possibly causing the observed effects, as has been reported previously (Beer et al., 2012; Lubick, 2008; Park et al., 2010; Pratsinis et al., 2013; Wang et al., 2014). The release of ions increases with decreasing particle size due to their relatively larger surface area.

There are two important points of consideration regarding the interpretation of the results of this study. First, the particle surface area in this study was estimated and not measured. Using Palas spark generation, particles are generated with a size distribution. By using the median particle size to estimate the particle surface area, the estimation introduces some uncertainties. Second, the silver nanoparticles in this study were generated using two different methods to be able to include a larger particle size than 65 nm. The larger particles of 160 nm were generated by nebulizing a dispersion with PVP coated 80 nm particles, while the smaller particles of 18, 34 and 60 nm were spark generated. As explained in the methods section, the larger particles were led through an oven which removed the PVP coating (Du et al., 2006; Peniche et al., 1993) and melted the particles into the single spherical particles depicted in Figure S1. However, the difference in generation method might have influenced the chemical composition of the nanoparticles by, for example, differences in the oxidation of the particles. Silver can oxidize in air, although at a slow rate. We believe it is unlikely that silver oxide was formed in the Palas spark generation setup, but we cannot exclude the possibility. There was no oxygen present at the position of the electrodes, it was added later on. In addition, at temperatures above 195 °C, the silver oxidation is reversed and silver oxide splits up in silver and oxygen (Franek, 2001), and the temperature of the oven was 700 °C. Therefore, we assume the particles were all similar apart from their diameter. Even though we estimated the particle surface area and we used two different generation methods to produce silver nanoparticles of four different sizes, the results of all the different sizes (including the largest particle size) show that the effects of silver nanoparticles after short-term inhalation can best be predicted by their total surface area that reaches the alveoli.

The data presented here confirm previous reports in which the total administered surface area appeared to be the best predictor for particles with the same chemical composition but of different size (Braakhuis et al., 2014b; Duffin et al., 2007; Ho et al., 2011; Horie et al., 2012; Kobayashi et al., 2009; Oberdorster et al., 2000; Stoeger et al., 2006). These papers show some evidence that based on the exposed dose; surface area might be a better dose metric to describe the effect of a range of nanoparticles, with the same chemical composition but differing in size, compared to mass. However, they did not take the internal dose in the lungs into account. For intratracheal instillation, one could assume the total bolus reaches the lungs, but in nose-only or whole-body chamber inhalation, the internal dose in the lungs should be measured. It should be noted that high dose rate methods such as intratracheal instillation, elicit significantly greater inflammation compared to low dose rate delivery such as nose-only or whole-body inhalation (Baisch et al., 2014). In the present study, based on the exposure concentration, surface area does bring the dose–response curves of the different particle sizes more towards each other, but the alveolar dose gives almost completely overlapping dose–response curves when surface area as a dose metric is used (Figure 7), showing the importance of using the alveolar dose instead of the external exposure concentrations.

To confirm whether the estimated alveolar dose expressed as surface area is a suitable dose descriptor also in other studies, we compared the results of the present study with the results of a previous short-term inhalation study with silver nanoparticles (Braakhuis et al., 2014a). In the previous study, 15 nm silver nanoparticles induced a doubling in the total cell number, a 175-fold increase in the number of neutrophils, and a 5-fold increase in the level of IL-1 β and MCP-1 at 24 h after the end of the exposure period (Braakhuis et al., 2014a). The mass exposure concentration was measured at 179 $\mu\text{g}/\text{m}^3$ and the estimated alveolar particle

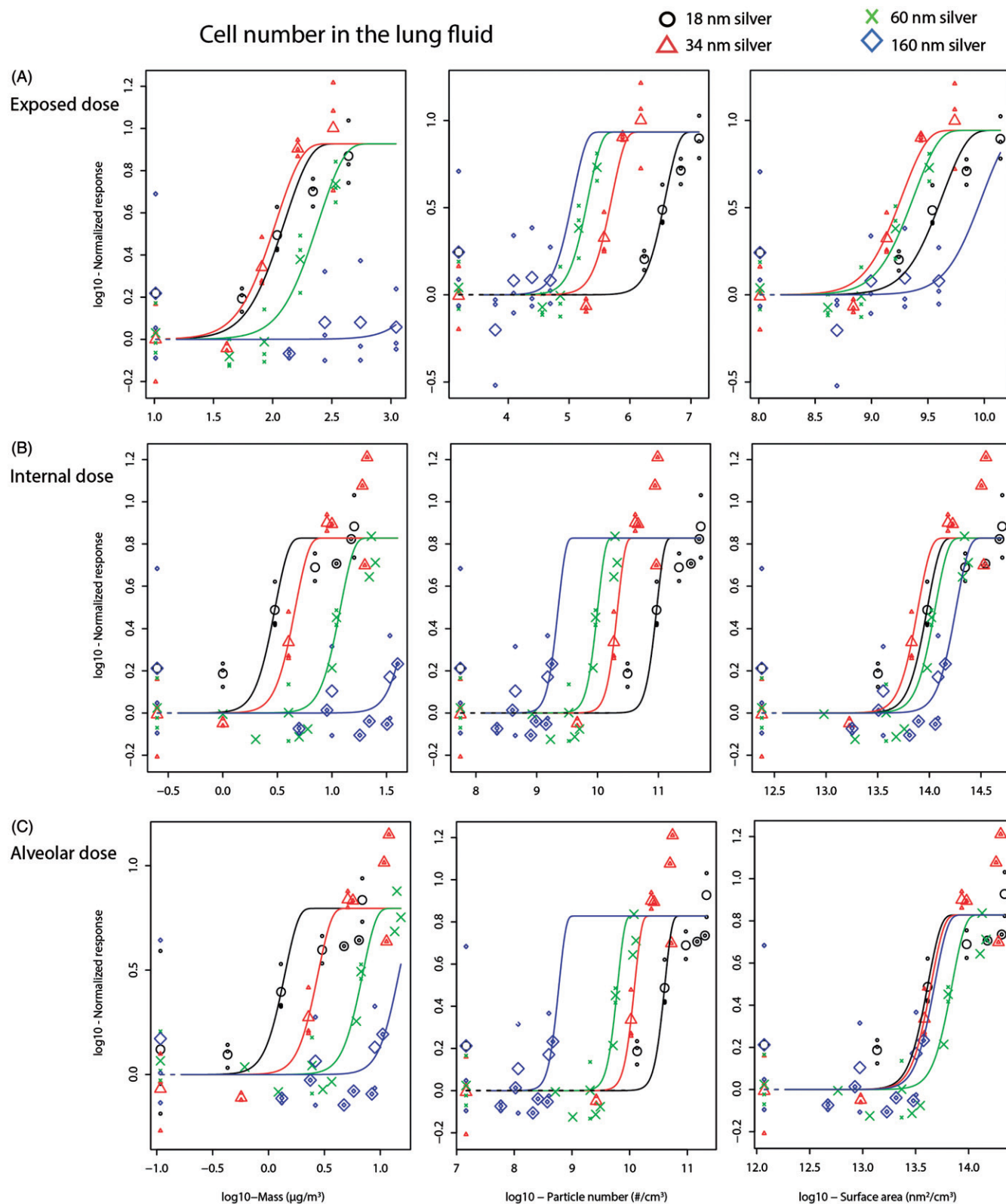


Figure 6. Total cell number in the BALF after inhalation exposure to different sizes of silver nanoparticles. The data are presented based on the measured silver concentration in the exposed air (A), the measured silver amount in the lungs (B) and the estimated silver amount in the alveoli (C). In addition, the data is presented based on mass (left), particle number (middle) and particle surface area (right). The small symbols represent individual animals and the larger symbols represent mean values of animals within the same dose-group.

surface area dose was $5.8 \times 10^{12} \text{ nm}^2/\text{cm}^3$ particles per mm^3 in the lungs. When compared to the results of the present study, the 18, 34, 60 and 160 nm particles induced these effects at mass exposure concentrations of 115, 91, 126 and $>1100 \mu\text{g}/\text{m}^3$, respectively, and at alveolar doses of $5.4 \times 10^{12} \text{ nm}^2/\text{cm}^3$ particles

per mm^3 in the lungs (ranging from 5.0 to $5.8 \times 10^{12} \text{ nm}^2/\text{cm}^3$). The alveolar doses expressed as particle surface area are similar in both studies, confirming that this is a suitable dose metric. Therefore, we recommend that internal alveolar doses are used in studies aimed at finding suitable dose metrics.

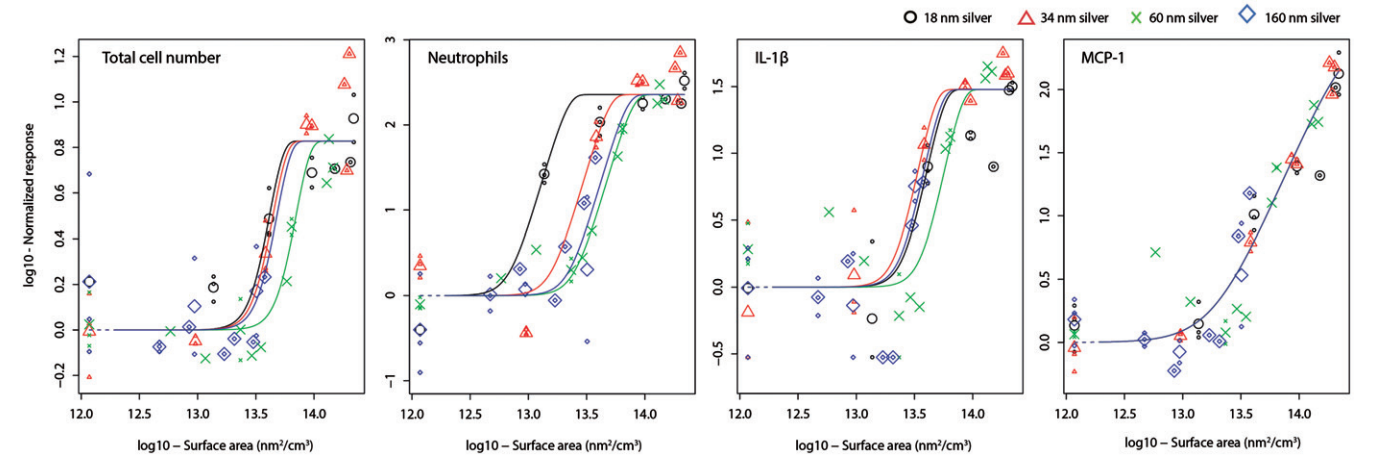


Figure 7. Total cell number, number of neutrophils, IL-1 β and MCP-1 in the BALF at 24h after inhalation exposure to different sizes of silver nanoparticles based on the particle surface area dose in the alveoli. All particle sizes show overlapping dose-dependent increases in the total cell number, number of neutrophils, IL-1 β and MCP-1 in the BALF. The small symbols represent individual animals and the larger symbols represent mean values of animals within the same dose-group.

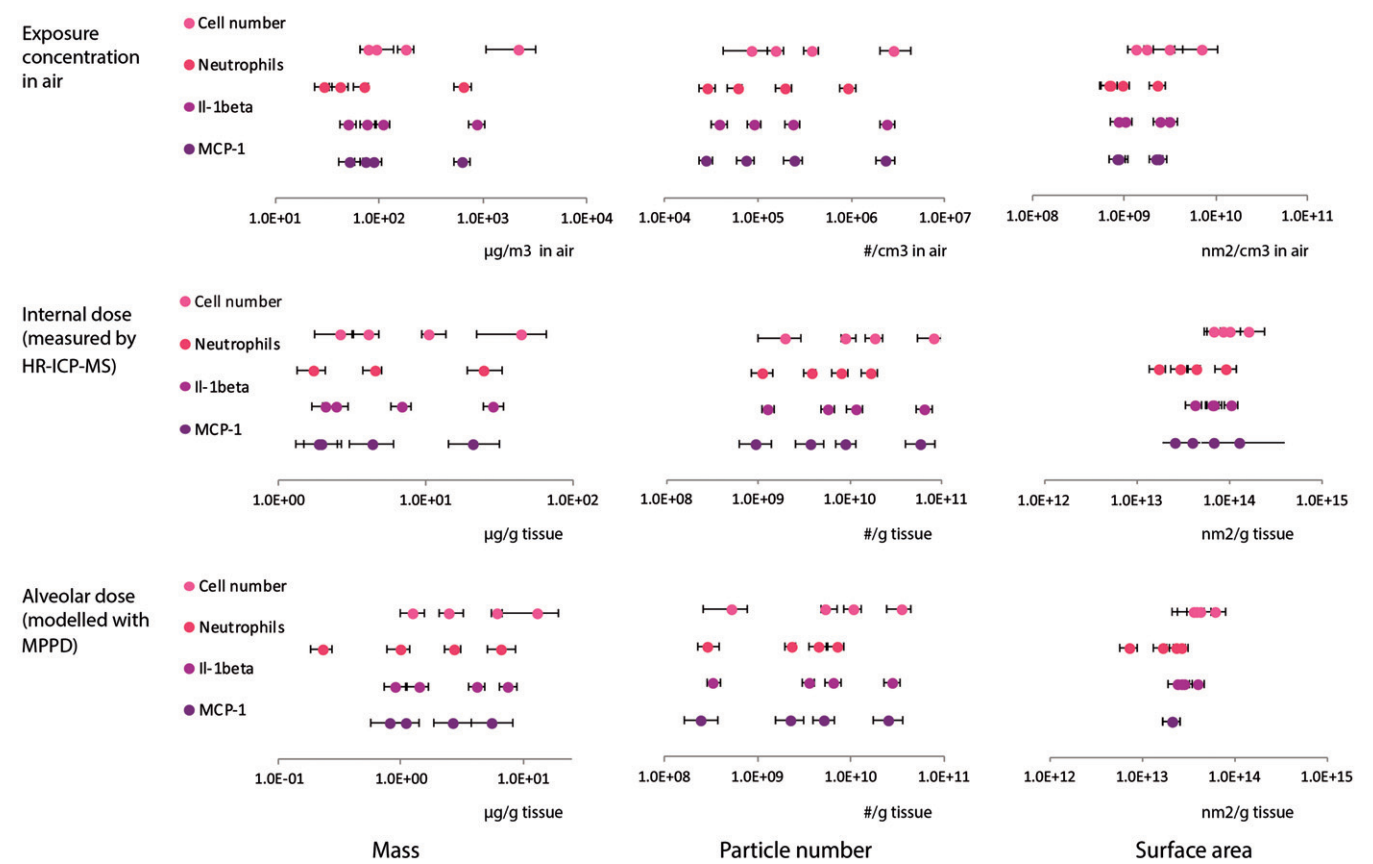


Figure 8. Critical effect doses for silver nanoparticles inducing a 20% increase in the total cell number, the number of neutrophils and the level of IL-1 β and MCP-1 in the bronchoalveolar lavage fluid compared to the controls (CED₂₀). The error bars represent a 95% confidence interval of the CED₂₀. The figure shows that the CED₂₀ of different sized silver nanoparticles after inhalation is similar when the dose is expressed as the total surface area of the silver nanoparticles that reach the alveoli.

We measured the amount of silver in the lungs at 24 h and 7 days after the end of the exposure period. Probably, there was some clearance from the lung of the (nano)particles between the end of exposure and the sacrifice at 24 h after exposure and after each day of exposure. According to literature, single nanoparticles and agglomerates of <100 nm are less efficiently phagocytized by alveolar macrophages compared to microparticles or large agglomerates of >1 μ m (Bakand et al., 2012; Muhlfeld et al., 2008; Oberdorster & Pott, 1987; Phalen et al., 2010) and less

efficiently cleared by mucociliary clearance (Geiser et al., 2008; Geiser & Kreyling, 2010; Oberdorster & Pott, 1987). Our results show similar amounts of silver (based on mass) in the lungs at 24 h after exposure to all four particle sizes. When we compare the amount of silver at 7 days after exposure to the amount at 24 h after exposure, we can calculate the clearance rate for the different particle sizes. In contrast to the literature that reports slower clearance of poorly soluble nanoparticles compared to larger particles, the clearance from the lungs was

the lowest for the 160 nm particles, i.e. the largest particles in our experiments. This discrepancy might be explained by (a) increased clearance from the lungs of the smaller particle sizes by translocation and (b) by (size/surface area dependent) dissolution of silver nanoparticles into ions that are more easily cleared compared to particles. The larger particles were generated by nebulizing a dispersion with PVP coated 80 nm particles, while the smaller particles were spark generated. One could argue that this may account for some of the differences found in the effects between the particles. However, all particles were led through an oven which removed the PVP coating (Du et al., 2006; Peniche et al., 1993) and melted the particles into the single spherical particles depicted in Figure S1. We assume, therefore, that the particles were all similar apart from their diameter. The difference in diameter will influence the dissolution rate of the silver particles since the dissolution rate and release of ions is proportional to the diameter of the particles (Ma et al., 2012). We also noted a size-dependent translocation of silver into the liver, with the smallest amounts for the largest particles. In the present study, the amount of silver in the liver decreased at 7 days after exposure compared to 24 h after exposure, indicating that silver is cleared from the liver and probably only accumulates to a limited extent, depending on the frequency of exposure. The potency of silver to accumulate in organs or tissues of the body should be investigated in experiments using long-term exposure to low concentrations of silver nanoparticles, resembling realistic exposure scenarios for humans.

The present study focused on the short-term inhalation of silver (nano)particles and showed that alveolar dose expressed as particle surface area seems the most suitable dose descriptor for the acute effects of silver nanoparticles across a range of sizes. For the risk assessment of silver nanoparticles, this dose metric can be used to predict the acute effects of comparable, uncoated silver nanoparticles that not have been tested in inhalation studies. Regarding long-term inhalation or chronic effects, the dose descriptor might be different since the kinetics of the silver nanoparticles and dissolution behaviour will play a role in the distribution of silver to other organs or tissues of the body where they might induce toxicity that is not directly correlated to the internal alveolar dose. For nanoparticles that differ from the silver nanoparticles tested in this study, for example, other chemical composition, shape or coating, the most suitable dose descriptor can be different because of differences in kinetics and mechanisms that might induce toxicity. In other words, it needs to be determined to what extent these results can be generalized.

Here, the dose descriptor was identified by distinguishing kinetics and toxicity. First, the particles that reach the effect site, i.e. the alveoli, were estimated. Subsequently, effects were related to different dose metrics of the alveolar dose. It may be that this approach is much broader applicable: some particle characteristics may have a major impact on kinetic processes, whereas other particle characteristics are important for inducing an effect. As a consequence, when the dose metric is investigated in view of external dose, different findings may occur, based on the interaction between kinetics and toxicity. Distinguishing kinetics and toxicity by determination of the particle characteristics at the effect site may help in understanding the mechanisms underlying a suitable dose metric, and thus aid in understanding and applying such information.

Conclusion

According to the results of the present study, the most suitable dose metric to describe the effect of silver nanoparticles after short-term inhalation is the surface area dose that reaches the alveoli. This dose metric can be used in the risk assessment of

silver nanoparticles to predict the acute effects of silver nanoparticles with unknown pulmonary toxicity and to derive exposure limits.

Acknowledgements

We would like to thank Ilse Gosens and John Boere for their help with the experimental design and Harry van Steeg for critical review of the manuscript. We thank Piet K. Beekhof for the analysis of the total protein, LDH and glutathione, and Henny W. Verharen, Hans J.C. Strootman, Ron F. Vlug, Christine M.R. Soputan, Jan Bos, Jolanda Rigters for their excellent technical assistance. In addition, we thank Jose van den Dungen for assistance with sample pretreatments and Chris T. W. M. Schneijdenberg for the assistance with the SEM imaging.

Declaration of interest

The authors declare that they have no competing interests.

This work was supported by the project “Integrated Risk Assessment of Nanomaterials” from the National Institute for Public Health and the Environment and by the NanoNextNL program “Risk Analysis and Technology Assessment: Human Health Risks”.

References

- Anjilvel S, Asgharian B. 1995. A multiple-path model of particle deposition in the rat lung. *Fundam Appl Toxicol* 28:41–50.
- Asgharian B, Price O, Miller F, Subramaniam R, Cassee FR, Freijer J, et al. 2009. Multiple-path particle dosimetry model (MPPD v 2.11): a model for human and rat airway particle dosimetry. In: *Applied Research Associates (ARA), H. I. F. H. S., National Institute for Public Health and the Environment (RIVM), and Ministry of Housing, Spatial Planning and the Environment (ed.) V2.11 ed. Raleigh, North Carolina, USA: Applied Research Associates (ARA).*
- Baisch BL, Corson NM, Wade-Mercer P, Gelein R, Kennell AJ, Oberdorster G, Elder A. 2014. Equivalent titanium dioxide nanoparticle deposition by intratracheal instillation and whole body inhalation: the effect of dose rate on acute respiratory tract inflammation. *Part Fibre Toxicol* 11:5–20.
- Bakand S, Hayes A, Dechsakulthorn F. 2012. Nanoparticles: a review of particle toxicology following inhalation exposure. *Inhal Toxicol* 24: 125–35.
- Barlow S, Chesson A, Collins JD, Flynn A, Hardy A, Jany K, et al. 2009. Use of the benchmark dose approach in risk assessment. *EFSA J* 1150:1–72.
- Beer C, Foldbjerg R, Hayashi Y, Sutherland DS, Autrup H. 2012. Toxicity of silver nanoparticles – nanoparticle or silver ion? *Toxicol Lett* 208: 286–92.
- Braakhuis HM, Gosens I, Krystek P, Boere J, Cassee FR, Fokkens P, et al. 2014a. Particle size dependent deposition and pulmonary inflammation after short-term inhalation of silver nanoparticles. *Part Fibre Toxicol* 11:49.
- Braakhuis HM, Park MV, Gosens I, de Jong WH, Cassee FR. 2014b. Physicochemical characteristics of nanomaterials that affect pulmonary inflammation. *Part Fibre Toxicol* 11:18–42.
- Cassee FR, Muijsers H, Duistermaat E, Freijer JJ, Geerse KB, Marijnissen JC, Arts JH. 2002. Particle size-dependent total mass deposition in lungs determines inhalation toxicity of cadmium chloride aerosols in rats. Application of a multiple path dosimetry model. *Arch Toxicol* 76: 277–86.
- Cho WS, Duffin R, Thielbeer F, Bradley M, Megson IL, Macnee W, et al. 2012. Zeta potential and solubility to toxic ions as mechanisms of lung inflammation caused by metal/metal oxide nanoparticles. *Toxicol Sci* 126:469–77.
- Du YK, Yang P, Mou ZG, Hua NP, Jiang L. 2006. Thermal decomposition behaviors of PVP coated on platinum nanoparticles. *J Appl Polym Sci* 99:23–6.
- Duffin R, Tran L, Brown D, Stone V, Donaldson K. 2007. Proinflammatory effects of low-toxicity and metal nanoparticles in vivo and in vitro: highlighting the role of particle surface area and surface reactivity. *Inhal Toxicol* 19:849–56.
- EFSA. 2009. Guidance of the Scientific Committee on a request from EFSA on the use of the benchmark dose approach in risk assessment. *EFSA J* 1150:1–72.

- Franek J. 2001. Temperature Dependence of Silver Oxide Formation. Minnesota: University of Minnesota.
- Geiser M, Casaulta M, Kupferschmid B, Schulz H, Semmler-Behnke M, Kreyling W. 2008. The role of macrophages in the clearance of inhaled ultrafine titanium dioxide particles. *Am J Respir Cell Mol Biol* 38: 371–6.
- Geiser M, Kreyling WG. 2010. Deposition and biokinetics of inhaled nanoparticles. *Part Fibre Toxicol* 7:2–18.
- Gerlofs-Nijland ME, Dormans JA, Bloemen HJ, Leseman DL, Boere JAF. 2007. Toxicity of coarse and fine particulate matter from sites with contrasting traffic profiles. *Inhal Toxicol* 19:1055–69.
- Gosens I, Mathijssen LE, Bokkers BG, Muijsers H, Cassee FR. 2014. Comparative hazard identification of nano- and micro-sized cerium oxide particles based on 28-day inhalation studies in rats. *Nanotoxicology* 8:643–53.
- Ho M, Wu KY, Chein HM, Chen LC, Cheng TJ. 2011. Pulmonary toxicity of inhaled nanoscale and fine zinc oxide particles: mass and surface area as an exposure metric. *Inhal Toxicol* 23:947–56.
- Horie M, Fukui H, Endoh S, Maru J, Miyauchi A, Shichiri M, et al. 2012. Comparison of acute oxidative stress on rat lung induced by nano and fine-scale, soluble and insoluble metal oxide particles: NiO and TiO₂. *Inhal Toxicol* 24:391–400.
- Kent RD, Vikesland PJ. 2012. Controlled evaluation of silver nanoparticle dissolution using atomic force microscopy. *Environ Sci Technol* 46: 6977–84.
- Kobayashi N, Naya M, Endoh S, Maru J, Yamamoto K, Nakanishi J. 2009. Comparative pulmonary toxicity study of nano-TiO₂ particles of different sizes and agglomerations in rats: different short- and long-term post-instillation results. *Toxicology* 264:110–18.
- Krystek P. 2012. A review on approaches to biodistribution studies about gold and silver engineered nanoparticles by inductively coupled plasma mass spectrometry. *Microchem J* 105:39–43.
- Krystek P, Braakhuis HM, Park MVDZ, Jong WHD. 2013. Inductively Coupled Plasma-mass Spectrometry in biodistribution Studies of (engineered) Nanoparticles. *Encyclopedia of Analytical Chemistry*. Hoboken, NJ: John Wiley & Sons, Ltd.
- Landsiedel R, Ma-Hock L, Kroll A, Hahn D, Schnekenburger J, Wiench K, Wohlleben W. 2010. Testing metal-oxide nanomaterials for human safety. *Adv Mater* 22:2601–27.
- Leo BF, Chen S, Kyo Y, Herpoldt KL, Terrill NJ, Dunlop IE, et al. 2013. The stability of silver nanoparticles in a model of pulmonary surfactant. *Environ Sci Technol* 47:11232–40.
- Lubick N. 2008. Nanosilver toxicity: ions, nanoparticles – or both? *Environ Sci Technol* 42:8617.
- Ma-Hock L, Strauss V, Treumann S, Kuttler K, Wohlleben W, Hofmann T, et al. 2013. Comparative inhalation toxicity of multi-wall carbon nanotubes, graphene, graphite nanoplatelets and low surface carbon black. *Part Fibre Toxicol* 10:23–42.
- Ma R, Levard C, Marinakos SM, Cheng Y, Liu J, Michel FM, et al. 2012. Size-controlled dissolution of organic-coated silver nanoparticles. *Environ Sci Technol* 46:752–9.
- Muhlfeld C, Gehr P, Rothen-Rutishauser B. 2008. Translocation and cellular entering mechanisms of nanoparticles in the respiratory tract. *Swiss Med Wkly* 138:387–91.
- Nanotechnologies POE. 2014. Consumer products inventory. [Online] Available at: <http://www.nanotechproject.org/cpi>. Accessed on June 2014.
- Oberdorster G, Finkelstein JN, Johnston C, Gelein R, Cox C, Baggs R, Elder AC. 2000. Acute pulmonary effects of ultrafine particles in rats and mice. *Res Rep Health Eff Inst* 96:5–74; disc 75–86.
- Oberdorster G, Pott F. 1987. Extrapolation from rat studies with environmental tobacco smoke (ETS) to humans: comparison of particle mass deposition and of clearance behavior of ETS compounds. *Toxicol Lett* 35:107–12.
- Park EJ, Yi J, Kim Y, Choi K, Park K. 2010. Silver nanoparticles induce cytotoxicity by a Trojan-horse type mechanism. *Toxicol In Vitro* 24: 872–8.
- Park MV, Annema W, Salvati A, Lesniak A, Elsaesser A, Barnes C, et al. 2009. In vitro developmental toxicity test detects inhibition of stem cell differentiation by silica nanoparticles. *Toxicol Appl Pharmacol* 240: 108–16.
- Pauluhn J. 2009. Pulmonary toxicity and fate of agglomerated 10 and 40 nm aluminum oxyhydroxides following 4-week inhalation exposure of rats: toxic effects are determined by agglomerated, not primary particle size. *Toxicol Sci* 109:152–67.
- Peniche C, Zaldivar D, Pazos M, Paz S, Bulay A, San Roman J. 1993. Study of the thermal degradation of poly(*N*-vinyl-2-pyrrolidone) by thermogravimetry-FTIR. *J Appl Polym Sci* 50:485–93.
- Phalen RF, Mendez LB, Oldham MJ. 2010. New developments in aerosol dosimetry. *Inhal Toxicol* 22:6–14.
- Pratsinis A, Hervella P, Leroux JC, Pratsinis SE, Sotiriou GA. 2013. Toxicity of silver nanoparticles in macrophages. *Small* 9:2576–84.
- RIVM. 2014. PROAST: software for dose–response modeling and benchmark dose analysis. PROAST38. 9 edn. Bilthoven, The Netherlands.
- Roursgaard M, Poulsen SS, Poulsen LK, Hammer M, Jensen KA, Utsunomiya S, et al. 2010. Time–response relationship of nano and micro particle induced lung inflammation. Quartz as reference compound. *Hum Exp Toxicol* 29:915–33.
- SCENIHR. 2010. Basis for the definition of the term ‘nanomaterial’. Brussels, Belgium: European Commission.
- Schinwald A, Murphy FA, Jones A, Macnee W, Donaldson K. 2012. Graphene-based nanoplatelets: a new risk to the respiratory system as a consequence of their unusual aerodynamic properties. *ACS Nano* 6:736–46.
- Slob W. 2002. Dose–response modeling of continuous endpoints. *Toxicol Sci* 66:298–312.
- Slob W. 2014a. Benchmark dose and the three Rs. Part I. Getting more information from the same number of animals. *Crit Rev Toxicol* 44: 557–67.
- Slob W. 2014b. Benchmark dose and the three Rs. Part II. Consequences for study design and animal use. *Crit Rev Toxicol* 44:568–80.
- Stebounova LV, Guio E, Grassian VH. 2011. Silver nanoparticles in simulated biological media: a study of aggregation, sedimentation, and dissolution. *J Nanopart Res* 13:233–44.
- Stoeger T, Reinhard C, Takenaka S, Schroepel A, Karg E, Ritter B, et al. 2006. Instillation of six different ultrafine carbon particles indicates a surface area threshold dose for acute lung inflammation in mice. *Environ Health Perspect* 114:328–33.
- van Ravenzwaay B, Landsiedel R, Fabian E, Burkhardt S, Strauss V, Ma-Hock L. 2009. Comparing fate and effects of three particles of different surface properties: nano-TiO₂(2), pigmentary TiO₂(2) and quartz. *Toxicol Lett* 186:152–9.
- Wang X, Ji Z, Chang CH, Zhang H, Wang M, Liao YP, et al. 2014. Use of coated silver nanoparticles to understand the relationship of particle dissolution and bioavailability to cell and lung toxicological potential. *Small* 10:385–98.
- Warheit DB, Webb TR, Colvin VL, Reed KL, Sayes CM. 2007a. Pulmonary bioassay studies with nanoscale and fine-quartz particles in rats: toxicity is not dependent upon particle size but on surface characteristics. *Toxicol Sci* 95:270–80.
- Warheit DB, Webb TR, Reed KL, Frerichs S, Sayes CM. 2007b. Pulmonary toxicity study in rats with three forms of ultrafine-TiO₂ particles: differential responses related to surface properties. *Toxicology* 230:90–104.
- Warheit DB, Webb TR, Sayes CM, Colvin VL, Reed KL. 2006. Pulmonary instillation studies with nanoscale TiO₂ rods and dots in rats: toxicity is not dependent upon particle size and surface area. *Toxicol Sci* 91:227–36.
- Wijnhoven SWP, Peijnenburg WJGM, Herberts CA, Hagens WI, Oomen AG, Heugens EHW, et al. 2009. Nano-silver – a review of available data and knowledge gaps in human and environmental risk assessment. *Nanotoxicology* 3:109–44.
- Yeh HC, Schum GM, Duggan MT. 1979. Anatomic models of the tracheobronchial and pulmonary regions of the rat. *Anat Rec* 195: 483–92.
- Zhu MT, Feng WY, Wang B, Wang TC, Gu YQ, Wang M, et al. 2008. Comparative study of pulmonary responses to nano- and submicron-sized ferric oxide in rats. *Toxicology* 247:102–11.
- Zook JM, Long SE, Cleveland D, Geronimo CL, Maccuspie RI. 2011. Measuring silver nanoparticle dissolution in complex biological and environmental matrices using UV–visible absorbance. *Anal Bioanal Chem* 401:1993–2002.